

# Significance of Infill Density on Mechanical Performance in Fused Deposition Modeling

Muhammad Haseem Umer<sup>1</sup>, Muttey-ur-Rehman<sup>1</sup>, Simra Ali<sup>1</sup>, Areesha Raza<sup>1</sup>, Laiba Muzammil<sup>1</sup>,  
Muhammad Shoaib Ijaz<sup>1</sup>, Muhammad Bilal Khan<sup>1</sup>, Muhammad Qasim Zafar<sup>1,2\*</sup>

<sup>1</sup>Faculty of Mechanical Engineering, Ghulam Ishaq Khan Institute of Engineering Sciences and Technology, Topi 23640, Pakistan

<sup>2</sup>State Key Laboratory of Tribology Department of Mechanical Engineering Tsinghua University, Beijing 100084 People's Republic of China

\*Corresponding Author: Muhammad Qasim Zafar ([muhhammadqasimzafar@gmail.com](mailto:muhhammadqasimzafar@gmail.com))

**Abstract-** Fused deposition modeling (FDM) is a widely employed additive manufacturing (AM) technique owing to its affordability and availability of equipment and materials. Polylactic Acid (PLA) is one of the most widely used materials due to its low cost, good mechanical properties, and biocompatibility. Mechanical performance is significantly influenced by FDM printing parameters. One of the most critical parameters that affect mechanical properties is infill density. In this study, standardized tests are used to ensure rigorous evaluations of the effects of different infill densities on PLA mechanical properties. Tensile strength, hardness, and impact strength are all considered in a comprehensive analysis. Results are then systematically compared with those of other commonly used FDM filaments, such as Acrylonitrile Butadiene Styrene (ABS) and High-density Polyethylene (HDPE). Through a rigorous experimental trial, we can analyze the effect of infill density on mechanical performance in FDM printing using PLA, ABS, and HDPE.

**Keywords:** Fused Deposition Modeling; Process Parameters; Infill Density; Mechanical Properties

## 1 Introduction

Additive manufacturing (AM) has completely revolutionized the manufacturing industry and it is quickly expanding its scope[1]. Beyond catalyzing advancements in manufacturing, additive manufacturing has spread its influence on other sectors as well, resulting in breakthroughs in the aerospace, construction, sports, and medicine sectors. This innovative approach not only allows for more complex geometries to be produced with greater precision but also facilitates product customization to meet the needs of the customer without incurring high customization fees. Additive manufacturing techniques offer all of this with less production time than subtractive manufacturing techniques, while also emphasizing environmental sustainability. The process of additive manufacturing is notably straightforward, comprising of following key steps:

1. Development of CAD model

2. Conversion of CAD model into a printable format
3. Slicing of the file using slicing software
4. Execution of the printing operation
5. Removal of supports (if necessary)
6. Performance of post-processing (if necessary)

While transforming various sectors, additive manufacturing has made significant progress as well and expanded over the years. To cover the wide range of additive manufacturing, the ASTM F42 committee has classified it into seven types as shown in Figure 1[2].



**Figure 1: AM Classification according to ASTM F42**

One particularly common and widely used type of additive manufacturing is material extrusion, which is also known as Fused filament fabrication (FFF) or fused deposition modeling (FDM). The material is extruded onto the print surface mostly a bed in a semi-molten form through a heated nozzle. The temperature at which the nozzle is heated is dependent on the material being processed. Figure 2 presents a schematic for the FDM process.

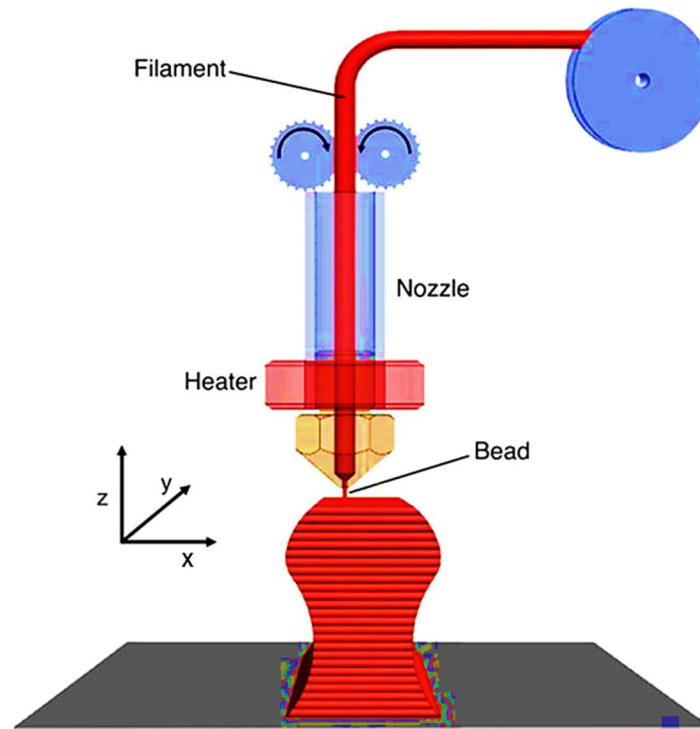


**Figure 2: Schematic Diagram of the FDM Process**

Due to its low cost and versatility, FDM is one of the 3D printing technologies that has attracted a wide range of industries, including automotive, aerospace, biomedical, and sports. Moreover, FDM takes center stage for creating patient-specific implants, revolutionizing personalized care by producing complex implants with superior dimensional accuracy. Mechanical properties refer to the physical characteristics of a material that determine its response to external forces or stresses. The fundamental mechanical properties encompass tensile strength, impact strength, flexural strength, shear strength, and hardness. The significance of these mechanical properties in Fused Deposition Modelling (FDM) becomes evident in diverse applications across aerospace, automotive, medical, and consumer product industries. In these sectors, the selection of additively manufactured parts with specific requirements for strength, durability, and safety underscores the critical role of mechanical properties. A significant challenge is the complexity of the process parameters, which directly affect the strength, quality, manufacturing, and performance efficiency of the developed components[3].

Layer thickness, build orientation, raster angle, nozzle temperature, printing speed, nozzle diameter, infill pattern, and infill density are important process parameters[4]–[6]. The influence of these process parameters has long been a source of interest for researchers[7]. In particular, this paper focuses on the effects of infill density, which characterizes the amount of solid required for 3D printing. The 3D printed objects are not solid throughout instead a hollow

structure with internal supports is made and infill density represents the ratio of the volume of material used to the total volume of the object. The value of infill density is set in the slicing software. Achieving the ideal infill density is crucial for 3D printing since it cuts down on both the cost of materials and printing time.

One of the advantages of FDM is its compatibility with a wide range of materials. One of the most commonly used FDM filaments is polylactic acid (PLA). PLA is one of the thermoplastics that is biodegradable and bioactive, which means it has a selective structural composition that causes it to induce any sort of biological process[8]. Therefore, opting for PLA specifically for our case study has to do with the positives that this material contains. PLA is bioactive and biocompatible, which makes it valuable in the pharmaceutical, healthcare, and biogenetics industries [9]. Most importantly, its source is renewable; which makes it an environment-friendly product. Not only this, but also PLA is well-known in the industries of packaging, textiles, and medical devices[10]. The use of PLA in industry necessitates the determination of mechanical properties. The purpose of this study is to determine the mechanical properties of PLA, as well as to investigate the effect of various infill densities on the mechanical properties of PLA and to compare it to other common FDM filaments.

## **2 Experimental Details**

### **2.1 3D Printer and Materials**

The specimens were produced using a CreatBot F430 machine with Polylactic Acid (PLA), Acrylonitrile Butadiene Styrene (ABS), and High-density polyethylene (HDPE)[11]. PLA is a biodegradable thermoplastic that also has bioactive properties. ABS is an amorphous polymer made up of three monomers: acrylonitrile, butadiene, and polystyrene. It possesses remarkable properties such as impact, heat, chemical, dimensional stability, tensile strength, surface hardness, rigidity, and electrical characteristics. HDPE is another thermoplastic polymer with high strength and chemical resistance. It is widely used in a variety of industries, including packaging, construction, and automotive. The specimens were modeled using PTC Creo Parametric 9.0 software per standard specifications, and the design was saved in Stereolithography (STL). Subsequently, the STL file underwent slicing in Creatware, the associated slicing software to generate G codes for all experimental runs. The generation of G codes was carried out for the following configuration: layer height of 0.2 mm, raster angle of 0, rectilinear infill pattern, flat build orientation, and printing speed of 30 mm/min. PLA specimens were printed with three different infill densities: 70%, 80%, and 100%. Meanwhile, ABS and HDPE specimens were printed with a constant infill density of 100%. Distinct nozzle

temperatures were employed for each material, including 210°C for PLA, 240°C for ABS, and 250°C for HDPE. The printing of specimens was carried out in compliance with these mentioned printing parameters.

## 2.2 Mechanical Testing

Tensile, hardness, and impact tests were performed on Polylactic Acid (PLA) at infill densities of 70%, 80%, and 100%. The purpose of this study was to examine how various infill densities (ID) affected the mechanical characteristics of PLA. To compare the PLA samples printed at 100% ID, comparable tensile, hardness, and impact tests were also conducted on ABS and HDPE at 100% infill densities. All tests followed the relevant ASTM guidelines[2].

Following the ASTM standards for tensile testing, D638[12], a dog bone sample was designed to the standard dimensions: thickness (3.20mm), width (13.11mm), and length (57.00mm). This was tested using an INSTRON TENSILE TESTING MACHINE. The tensile specimen placed in between holders is shown in Figure 3. In this, the sample experienced deformation until it fractured as a result of the load being applied gradually.



**Figure 3: Tensile Testing using Instron Tensile Testing Machine**

For hardness testing, a square-shaped specimen with a thickness of 6.35mm and a length of 25.4mm was created following ASTM standard D785[13]. The samples were tested on the DIGITAL ROCKWELL HARDNESS TESTING MACHINE as illustrated in Figure 4. This involves applying a gradual load using a steel ball as an indenter, which creates an indent in the specimen's center.



**Figure 4: Hardness Testing using Rockwell Hardness Testing Machine**

As per ASTM standard D256, specimens with dimensions of 55 mm in length, 12.7 mm in width, and 3 mm in thickness were subjected to impact testing. Each specimen featured a 45-degree notch in the center for controlled impact testing. The state-of-the-art SKIMADU CHARPY IMPACT TESTING MACHINE was employed to perform the impact strength evaluations. The specimens were tested by placing them horizontally on the sample holder and subjecting them to the impact force produced by a 2.245 kg moving hammer that swung like a pendulum as also presented in Figure 5.

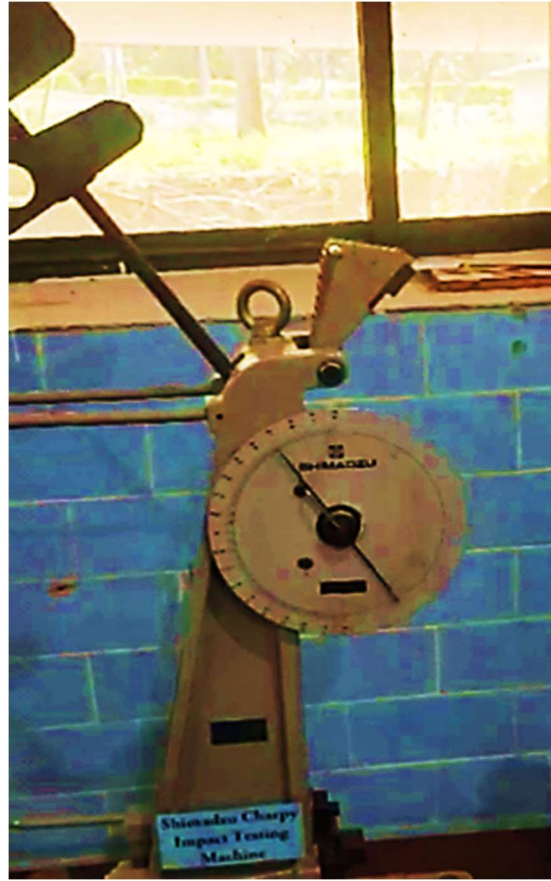


**Figure 5: Impact Testing using SKIMADU Charpy Impact Testing Machine**

The relevant formula was then used to calculate the Charpy impact value, which yielded an accurate measurement of material toughness. The formula used for Charpy energy calculation is provided as follows [12]:

$$E = mgh (\cos \beta - \cos \alpha) \quad (1)$$

Where E is the energy absorbed by the specimen of area A, m is the mass of the hammer, h is the height from which the hammer is released,  $\alpha$  is the angle of release and  $\beta$  donates the after-strike angle. The impact strength (IS) is provided by the following expression [12].

$$IS = E/A \quad (2)$$

The nomenclature for the specimen designed is presented in Table 1.

**Table 1: Nomenclature for specimen**

Designation	Material	Infill Density	Test
PLA70T	PLA	70	Tensile
PLA80T	PLA	80	Tensile
PLA100T / PLA-T	PLA	100	Tensile
PLA70H	PLA	70	Hardness

PLA80H	PLA	80	Hardness
PLA100H / PLA-H	PLA	100	Hardness
PLA70I	PLA	70	Impact
PLA80I	PLA	80	Impact
PLA100I / PLA-I	PLA	100	Impact
ABS-T	ABS	100	Tensile
ABS-H	ABS	100	Hardness
ABS-I	ABS	100	Impact
HDPE-T	HDPE	100	Tensile
HDPE-H	HDPE	100	Hardness
HDPE-I	HDPE	100	Impact

### 3 Results and Discussion

The PLA, ABS, and HDPE specimens printed using CreatBot F430 were subjected to mechanical testing, including tensile, hardness, and impact tests as described in section 2.2. The subsequent sections present the results of the specimen testing.

#### 3.1 Tensile Test

Tensile testing was conducted on PLA specimens with varying infill densities, as well as on PLA, ABS, and HDPE specimens using an Instron tensile testing machine. The stress-strain curve was obtained as the result of the testing. These curves illustrate the impact of different infill densities on PLA and allow for a comparison between PLA, ABS, and HDPE.

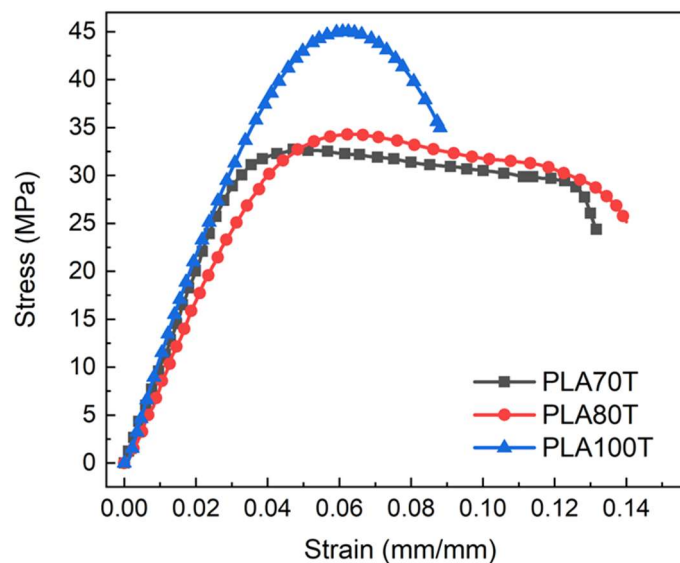


**Figure 6: Tensile Stress-Strain Curve for PLA specimens**

The tensile stress-strain curve for the PLA specimens is presented as follows in Figure 6. The results show the comparison of the PLA specimen with the varying infill densities. The results show that the sample with the 100% infill density presented the highest tensile strength and Young's modulus. The maximum Ultimate Tensile Strength (UTS) of 45.01 MPa was also indicated by the sample with 100% infill density. A more thorough examination, however, reveals that specimens with 70% and 80% infill densities exhibited better energy absorption than the one hundred percent infill density counterpart. In particular, the specimen with 100% infill density fractured at 0.088 mm/mm with minimal strain. By comparison, the specimen with an 80% infill density demonstrated a strain of 0.141 mm/mm, whereas the specimen with a 70% infill density indicated a strain of 0.132 mm/mm, suggesting a greater ability for deformation and absorption of energy.

Comparing the tensile characteristics of PLA with 100% infill density to those of ABS and HDPE with the same infill density is another significant study aspect. Examining the corresponding tensile stress-strain curves for each material helps with this comparative study. These stress-strain curves are shown graphically in Figure 7, which also highlights the variations in tensile behavior across the different materials.

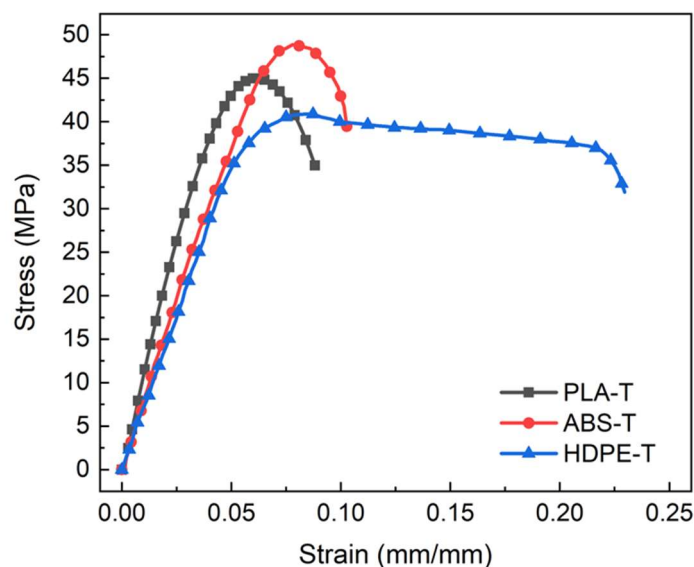


**Figure 7: Tensile Stress-Strain Curves for PLA, ABS, and HDPE specimens**

The stress-strain curve shows how the tested materials' tensile strength and Young's modulus varied. Particularly, the ABS specimen demonstrated the highest values for both parameters, while HDPE exhibited the lowest values for both tensile strength and Young's Modulus. Notably, when compared to the other two specimens, the ABS specimen displayed the highest Ultimate Tensile Strength (UTS), measuring 48.87 MPa. Furthermore, investigation reveals that HDPE showed high energy absorption during tensile loading displaying a maximum

tensile strain of 0.229 mm/mm, while PLA and ABS displayed strains of 0.088 mm/mm and 0.103 mm/mm, respectively.

Table 2 displays the tensile test results, comparing and explaining the tensile characteristics of various specimens.

**Table 2: Tensile Properties of the specimens**

<b>Specimens</b>	<b>Yield Strength MPa</b>	<b>Young's Modulus GPa</b>	<b>Ultimate Tensile Strength (UTS) MPa</b>	<b>Maximum Strain mm/mm</b>
<b>PLA70T</b>	29.03	0.951	32.71	0.132
<b>PLA80T</b>	30.46	0.748	34,28	0.140
<b>PLA100T</b>	36.52	1.04	45.01	0.088
<b>ABS-T</b>	43.77	0.731	48.87	0.103
<b>HDPE-T</b>	34.88	0.693	40.89	0.229

### 3.2 Hardness Test

Comparable to the tensile test, the Rockwell hardness testing machine was used to test the hardness of PLA, ABS, and HDPE specimens as well as PLA specimens with various infill densities. The materials' hardness values, which are displayed in Table 3, were determined by the testing results.

**Table 3: Rockwell Hardness Value for specimens**

<b>Specimens</b>	<b>Rockwell Hardness RHA</b>
<b>PLA70T</b>	74.8
<b>PLA80T</b>	87
<b>PLA100T</b>	118
<b>ABS-T</b>	91
<b>HDPE-T</b>	122

To enhance comprehension of the impact of infill density on the Rockwell hardness value of PLA samples, a visual representation of the relationship between changes in infill density and the hardness properties of the PLA is provided by the bar graph in Figure 8. Hardness is observed to increase with an increase in infill density.

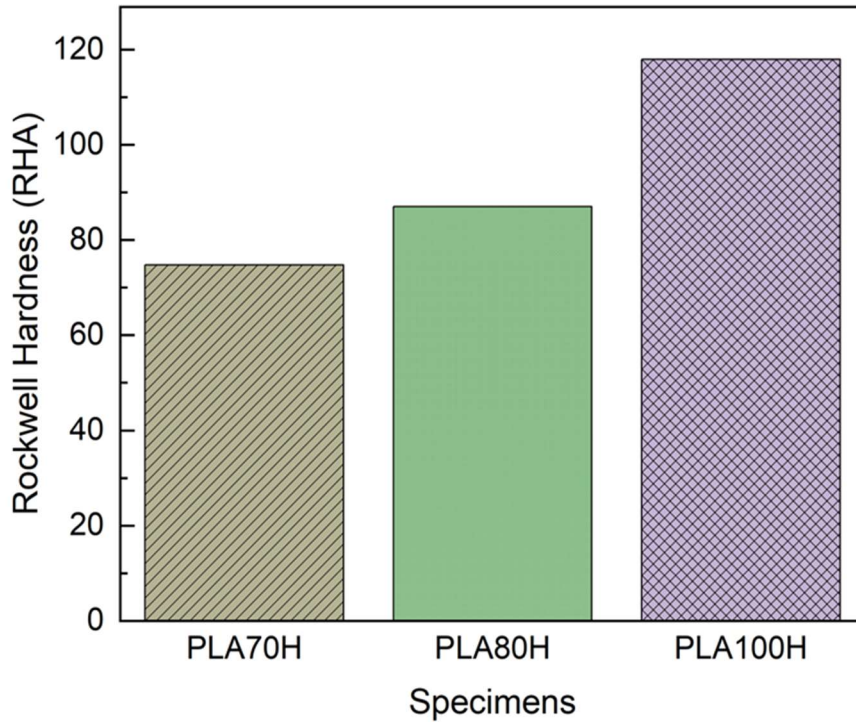


**Figure 8: Rockwell Hardness values for PLA specimens**

However, it still doesn't provide information on comparing the hardness values of various filament materials. Choosing the appropriate material for an application requires an understanding of the filaments' hardness properties. Remembering that the comparison is displayed as a bar graph in Figure 9. This demonstrates that the highest Rockwell hardness value is found in the ABS specimen, which is followed by PLA and then HDPE.

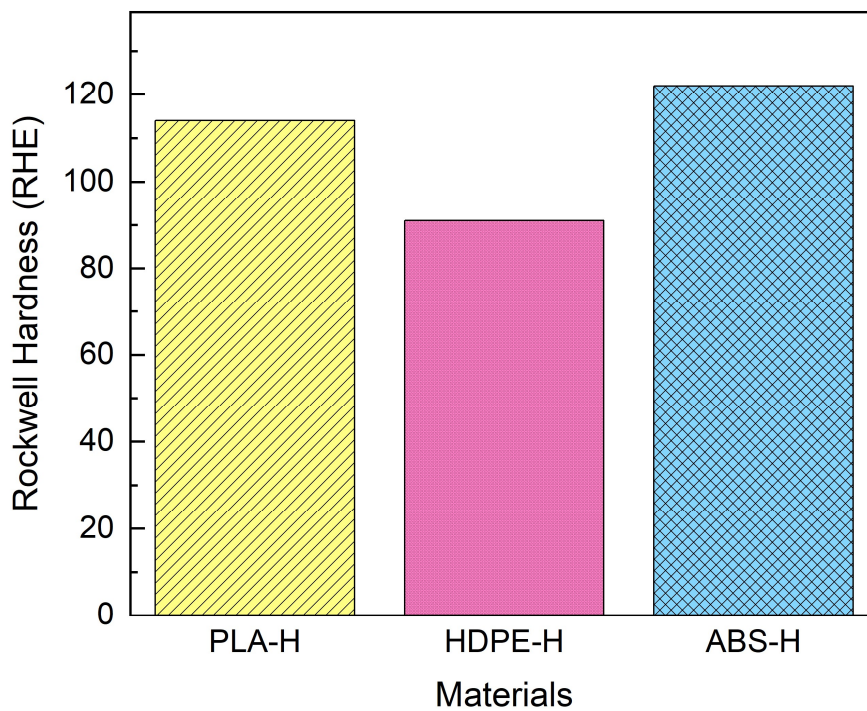


**Figure 9: Rockwell Hardness for PLA, HDPE, and ABS**

### 3.3 Impact Test

One of the key mechanical properties of the material that affects structural integrity is its impact strength. Determining the impact strength is therefore essential. The impact strength is calculated using equation (2), which is covered in section 2.2. Table 4 displays the impact strength values for each specimen derived from the mentioned equation.

**Table 4: Impact Strength for specimens**

Specimens	Impact Strength kJ/mm <sup>2</sup>
PLA70T	74.8
PLA80T	87
PLA100T	118
ABS-T	91
HDPE-T	122

To improve understanding of how infill density affects PLA sample impact strength values, Figure 10's bar graph illustrates the relationship between variations in infill density and PLA impact properties. The impact strength is observed to improve with the increase in infill density.

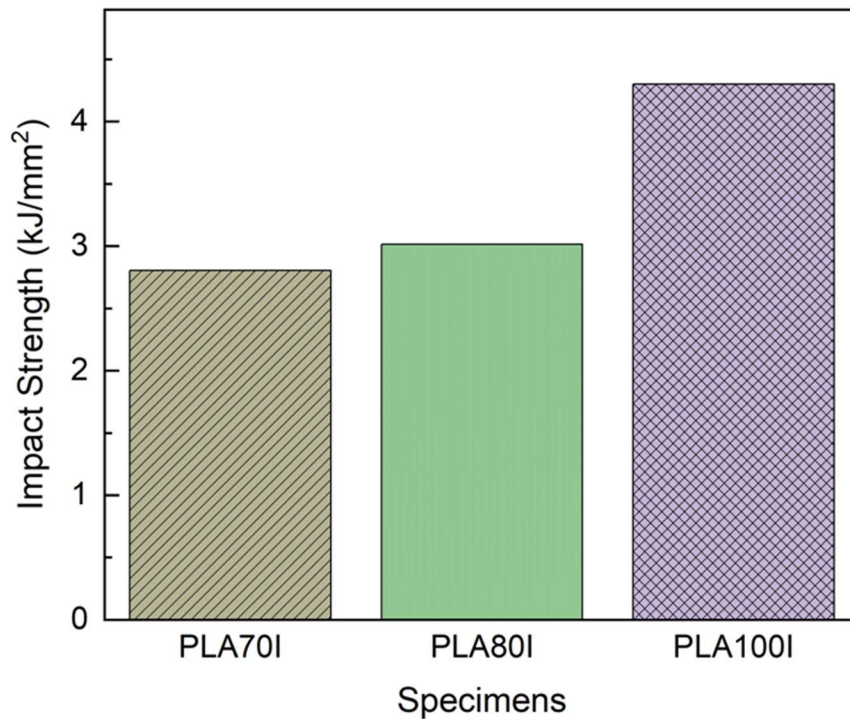


**Figure 10: Impact Strength values for PLA specimens**

On the other hand, it still lacks information about comparing the impact strength effect on different filament materials. Understanding the impact properties of the filaments is necessary to select the right material for a given application. Consideration that Figure 11 shows the comparison as a bar graph. This indicates that the ABS specimen has the maximum impact strength, followed by HDPE and then PLA.

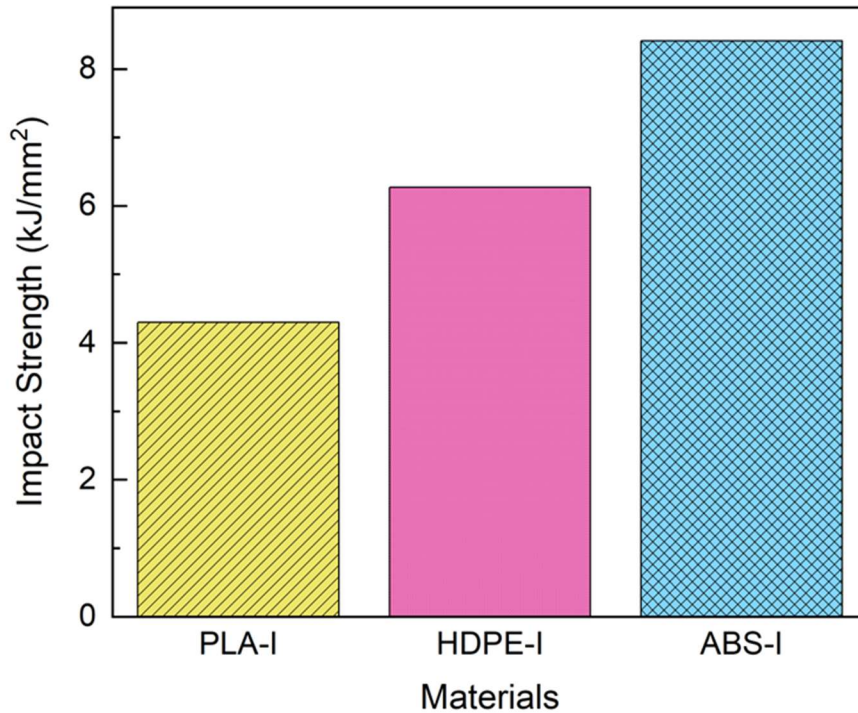


**Figure 11: Impact Strength for PLA, HDPE, and ABS**

#### **4 Conclusion**

The study assessed the mechanical characteristics of polylactic acid (PLA) at various infill densities, providing important insights regarding how infill densities affect the mechanical behavior of PLA. Additionally, it computed and displayed the mechanical strength of HDPE and ABS produced using Fused Deposition Modeling. The result section of this study highlights the following findings:

- As infill density increased, porosity and air gaps between layers decreased, creating a more compact and rigid structure that allowed the PLA specimens with high infill densities to achieve the maximum Rockwell hardness, impact strength, UTS, Young's Modulus, and tensile strength.
- The structures with lower infill densities had air gaps, which allowed for deformation within the layers. The specimen can absorb the crack under loading because of these air gaps, which prevent the crack from propagating. As a result, specimens showing

less infill density showed more strain and absorption of energy. Higher infill densities, on the other hand, were associated with compact layers devoid of porosity, which promoted unhindered crack propagation and reduced energy absorption.

- ABS outperformed HDPE and PLA in terms of mechanical properties such as hardness, impact strength, and tensile strength. Furthermore, the outcomes showed that PLA performed better in terms of Rockwell hardness and tensile properties than HDPE. PLA, on the other hand, lacked the impact resistance of HDPE.

Significant insights into the mechanical properties are presented by these results, allowing the appropriate filament materials and printing parameters to be selected for the specific applications.

### Acknowledgments

Corresponding author Muhammad Qasim Zafar would like to dedicate love and respect to a father whose belief in his son's potential continues to inspire and uplift, even in this absence.

### References:

- [1] M. Q. Zafar and H. Zhao, "4D Printing: Future Insight in Additive Manufacturing," *Metals and Materials International*, vol. 26, no. 5, pp. 564–585, 2020, doi: 10.1007/s12540-019-00441-w.
- [2] ISO/TC 261 and ASTM- Komitee F42, "ISO/ASTM 52900:2021," *Additive manufacturing — General principles — Fundamentals and vocabulary*, vol. 2. 2021.
- [3] M. S. Mustafa, M. A. Muneer, and M. Q. Zafar, "Process parameter optimization for Fused Filament Fabrication additive manufacturing of PLA / PHA biodegradable polymer blend," vol. 37, no. 1, pp. 1–14, 2022.
- [4] T. Koziar and C. Kundera, "Evaluation of the Influence of Parameters of FDM Technology on the Selected Mechanical Properties of Models," in *Procedia Engineering*, 2017. doi: 10.1016/j.proeng.2017.06.080.
- [5] T. Nancharaiah, "Optimization of Process Parameters in FDM Process Using Design of Experiments," *International Journal on Emerging Technologies 2(1):*, vol. 2, no. 1, 2011.
- [6] I. J. Solomon, P. Sevel, and J. Gunasekaran, "A review on the various processing parameters in FDM," in *Materials Today: Proceedings*, 2020. doi: 10.1016/j.matpr.2020.05.484.
- [7] E. Vahabli and S. Rahmati, "Improvement of FDM parts' surface quality using optimized neural networks - Medical case studies," *Rapid Prototyping Journal*, vol. 23, no. 4, 2017, doi: 10.1108/RPJ-06-2015-0075.
- [8] M. Hassan, A. K. Mohanty, and M. Misra, "3D printing in upcycling plastic and biomass waste to sustainable polymer blends and composites: A review," *Materials & Design*, vol. 237, p. 112558, Jan. 2024, doi: 10.1016/J.MATDES.2023.112558.

- [9] V. Andronov, L. Beránek, V. Krůta, L. Hlavůňková, and Z. Jeníková, “Overview and Comparison of PLA Filaments Commercially Available in Europe for FFF Technology,” *Polymers*, vol. 15, no. 14, 2023, doi: 10.3390/polym15143065.
- [10] J. M. Chacón, M. A. Caminero, E. García-Plaza, and P. J. Núñez, “Additive manufacturing of PLA structures using fused deposition modelling: Effect of process parameters on mechanical properties and their optimal selection,” *Materials and Design*, vol. 124, 2017, doi: 10.1016/j.matdes.2017.03.065.
- [11] C. M. González-Henríquez, M. A. Sarabia-Vallejos, and J. Rodríguez-Hernandez, “Polymers for additive manufacturing and 4D-printing: Materials, methodologies, and biomedical applications,” *Progress in Polymer Science*. 2019. doi: 10.1016/j.progpolymsci.2019.03.001.
- [12] ASTM, “ASTM E2248 – 18 Standard Test Method for Impact Testing of Miniaturized Charpy V-notch Specimens,” *ASTM*, 2021.
- [13] ASTM, “D785-03-Standard Test Method for Rockwell Hardness of Plastics and Electrical Insulating,” *Annual Book of ASTM Standards*, vol. 14, 2008.